Title

Unsupervised mRNA-seq classification of heart transplant endomyocardial biopsies.

Journal

Clinical Transplantation, 37(9)

Authors

Romero, Erick
Tabak, Esteban
Fishbein, Gregory
et al.

Publication Date

2023-09-01

DOI

10.1111/ctr.15011

HHS Public Access

Author manuscript

Clin Transplant. Author manuscript; available in PMC 2024 September 01.

Published in final edited form as:

Clin Transplant. 2023 September ; 37(9): e15011. doi:10.1111/ctr.15011.

Unsupervised mRNA-seq Classification of Heart Transplant Endomyocardial Biopsies

Erick Romero, MD MAS[1], **Esteban Tabak, PhD**[2], **Gregory Fishbein, MD**[3], **Silvio Litovsky, MD**[4], **Jose Tallaj, MD**[4], **David Liem, MD PhD**[1], **Maral Bakir, RN**[3], **Yeraz Khachatoorian, MD MPH**[5], **Brian Piening, PhD**[6], **Brendan Keating, PhD**[7], **Mario Deng, MD**[3], **Martin Cadeiras, MD**[1]

[1]Division of Cardiovascular Medicine, UC Davis Medical Center, Sacramento, CA

[2]Courant Institute of Mathematical Sciences, New York University, New York, NY

[3]David Geffen School of Medicine, UCLA Medical Center, Los Angeles, CA

[4]UAB School of Medicine, University of Alabama at Birmingham, Birmingham, AL

[5]Cardiology department, Westchester Medical Center, New York, NY

[6]Earle A. Chiles Research Institute, Providence, Portland, Oregon

[7]Department of Surgery, University of Pennsylvania, Perelman School of Medicine, PA

Abstract

Background—Endomyocardial biopsy (EMB) is currently considered the gold standard for diagnosing cardiac allograft rejection. However, significant limitations related to histological interpretation variability are well-recognized. We sought to develop a methodology to evaluate EMB solely based on gene expression, without relying on histology interpretation.

Methods—Sixty-four EMBs were obtained from 47 post-heart transplant recipients, who were evaluated for allograft rejection. EMBs were subjected to mRNA sequencing, in which an unsupervised classification algorithm was used to identify the molecular signatures that best classified the EMBs. Cytokine and natriuretic peptide peripheral blood profiling was also performed. Subsequently, we performed gene network analysis to identify the gene modules and gene ontology to understand their biological relevance. We correlated our findings with the unsupervised and histological classifications.

Results—Our algorithm classifies EMBs into three categories based solely on clusters of gene expression: unsupervised classes 1, 2, and 3. Unsupervised and histological classifications were

Correspondence Martin Cadeiras, MD, Division of Cardiovascular Medicine, UC Davis Medical Center, 4301 X St. Sacramento, CA 95817. (mcadeiras@ucdavis.edu, mcadeiras@gmail.com); Erick Romero, MD, Division of Cardiovascular Medicine, UC Davis Medical Center, 4301 X St. Sacramento, CA 95817, Sacramento, CA 95817. (esromero991@gmail.com).

Authorship

MC, ET, and MD conceived and designed the study; ET, GF, SL, JT, MB, ER, and MC acquired the data; ET, GF, ER, MC, DL, JT, BK, YK, BP, MC, and MD analyzed and interpreted the data; all authors contributed to drafting the manuscript; and all authors provided comments and approved the final version of the manuscript.

Disclosure

The authors declare no conflicts of interest.

closely related, with stronger gene module-phenotype correlations for the unsupervised classes. Gene ontology enrichment analysis revealed processes impacting on the regulation of cardiac and mitochondrial function, immune response, and tissue injury response. Significant levels of cytokines and natriuretic peptides were detected following the unsupervised classification.

Conclusion—We have developed an unsupervised algorithm that classifies EMBs into three distinct categories, without relying on histology interpretation. These categories were highly correlated with mitochondrial, immune, and tissue injury response. Significant cytokine and natriuretic peptide levels were detected within the unsupervised classification. If further validated, the unsupervised classification could offer a more objective EMB evaluation.

Data statement—The data that support the findings of this study are available from the corresponding author upon reasonable request.

Keywords

Endomyocardial biopsy; cardiac allograft rejection; acute cellular rejection; gene expression

INTRODUCTION

Despite major advances in heart transplantation, acute allograft rejection remains an important complication leading to cardiac allograft vasculopathy, graft failure, and death.[1–4] Endomyocardial biopsy (EMB) is considered the gold standard method for monitoring allograft rejection, and is classified according to the consensus criteria established by the International Society for Heart and Lung Transplantation (ISHLT).[5,6] However, EMB histological analyses can suffer from sampling errors, Quilty lesions, and most importantly, high rates of interpretation variability among pathologists.[7–10] Yet, to date the EMB remains the gold standard. This is a major obstacle, as it restricts progress in the field, hinders our comprehension of disease pathophysiology, and places patients at risk of receiving suboptimal diagnoses and treatments. Thus, there is a critical need for additional biomarkers and methods to improve or complement EMBs evaluations.

The analysis of EMBs at the molecular level has garnered attention as a means of enhancing diagnostic accuracy and shedding light on the molecular condition of the allograft. Intragraft gene expression profiling has been used to understand the molecular insights involved in allograft rejection and to improve the accuracy of diagnosis and classification of acute allograft rejection.[11–16] Gene expression profiling for diagnostic applications also has limitations, including the interpretation and reproduction of results due to the existence of confounding factors that increase the variability of the gene expression data, ranging from batch effects to patient-specific characteristics such as age, ethnicity, and variations in corticosteroid therapy which is known to influence gene expression post-transplant.[17–20] Therefore, it is important to develop methodologies that can help mitigate the impact of such confounding factors.

To address the interpretation variability of EMBs, the primary objective of this study was to develop an unsupervised molecular classification methodology based solely on EMB gene expression, without relying on histological interpretations, while also taking

confounding factors into consideration. We hypothesized that EMB has inherent gene expression signatures of allograft rejection that would guide EMB classification independent of histopathological assessment (unsupervised). To assess the reliability of traditional histological interpretations, we conducted an ISHLT grading agreement among pathologists. We employed the *optimal transport* methodology to classify EMBs in an unsupervised manner, while accounting for confounding factors.[21–23] In order to relate the developed classification to the clinical context, we analyzed its correlations with circulating B-type natriuretic peptide (BNP) and cytokines.

MATERIALS AND METHODS

Study design

In this pilot study, EMB were collected during routine surveillance or when clinically indicated and analyzed in a cross-sectional fashion. This study aimed to develop an unsupervised molecular classification of acute cellular-mediated rejection (ACR). Then, we investigated the relationship between the developed molecular classification and cytokines, BNP and standard ISHLT histological grades. Additionally, agreement between pathologists on ISHLT grading was also explored. An overview of the study design is shown in Figure 1.

Participants and EMB specimens

Patient EMB samples were obtained from the University of Alabama at Birmingham (UAB) and the University of California Los Angeles (UCLA). Data on demographics, site, rejection status, and clinical characteristics were obtained for each sample. The study was approved by the institutional review board (IRB) and all patients signed an informed consent form (UAB IRB F110707008; UCLA IRB 12–001164).

EMBs were performed using the standard transvenous technique. During the procedure, an appropriately sized cardiac specimen (~1.5 mm in diameter) was collected for study purposes. The specimens were immersed in TRIzol reagent and frozen in liquid nitrogen immediately after the procedure. For two patients with failed cardiac transplants, tissues were collected at the time of explant and processed following the same protocol. Biopsy hematoxylin-eosin-stained slides were reviewed by pathologists as required by the standard care protocol to score for allograft rejection, and Quilty effects using the ISHLT criteria.[5,6,8] In a blinded fashion, the same slides were provided in a digital format to two additional external pathologists, one from UCLA and one from UAB. The pathologists submitted their readings to the investigators for agreement analysis. The additional histopathological evaluation was used post-analysis of the mRNA-seq classification to interpret the results.

RNA sequencing

The tissue specimens were subjected to second-generation mRNA-seq. The samples were processed at either the UAB or UCLA core genomic facilities following a standard methodology. Agilent 2100 Bioanalyzer (Agilent Technologies, Palo Alto, CA) was used to assess the quality of the total mRNA. TruSeq library prep and HiSeq2000 sequencing were used for whole-genome next-generation mRNA-seq (Illumina, San Diego, CA, USA). The genome library consisted of random fragmentation of polyA mRNA followed by

cDNA production using random polymers. The cDNA libraries were quantified using qPC clusters to yield approximately 725 K-825 K clusters/mm^2. After the first base addition, the parameters were assessed, and the cluster density and quality were determined. Single-end sequencing was performed to align cDNA sequences with the reference genome. FASTQ files obtained from mRNA-seq were then imported into Strand NGS 2.1 (Agilent, Palo Alto, CA and Strand Life Sciences, Bengaluru, India) to align the raw reads to the human reference genome (hg19). The read counts were normalized using the DESeq algorithm.

Unsupervised Classification of EMBs using the optimal transport methodology

The approach utilized in this study was considered specifically for heart transplant rejection. The *optimal transport* methodology is an extension of the mathematical theory of optimal transport that filters potential factors known to influence gene expression and histology interpretation variability.[21,22,24] The clustering algorithm relies on flows in feature space for gene expression clustering and classification.[23] We have proposed this methodology and described in a previous heart transplant rejection report.[25] A detailed description of the methodology used to develop the unsupervised classification used in this project is provided in the Supplementary material. To assign classes to samples, we use optimal transport to control confounding factors from the expression. For each gene, optimal transport adjusted the expression based on the effect of age, sex, presence of a Quilty lesion, batch effect, and prednisone dose. Hence the variability left is only what is not explainable by the confounding factors. Next, we apply the flows in feature space clustering algorithm using the adjusted gene expression, which has two random components: the order in which genes are considered and small perturbations in initial class priors. In contrast to other methods, the utilized methodology permits the sequential diagnosis of samples, one at a time. Each sample is treated as a test case while the remaining samples are utilized for training. The number of clusters was determined based on optimal reproducibility, i.e. robustness under random initializations of the algorithm. Finally, we calculate the probability that each sample belongs to each class assuming a Gaussian distribution of gene expression within each class.

Cytokine profiling and natriuretic peptides

BNP was available at the time of biopsy for 30 samples. Peripheral blood specimens were obtained at the same time as cardiac biopsies for cytokine profiling for 19 samples. Serum cytokine profiling assay was performed on peripheral blood specimens. The cytokine assay procedures are provided in the Supplementary Material.

Statistical analysis

Statistical analysis was applied to examine differences in gene expression among the rejection groups as well as among the different unsupervised classes. To further understand the underlying molecular network, weighted gene co-expression network analysis (WGCNA), hub gene analysis, and gene ontology (GO) analysis were performed to identify important genes within biological networks. The analysis was performed using the WGCNA package implemented in R, Cytoscape, and the plugin CytoHubba.[26–28] We computed the eigengenes for each module and used the correlation between eigengenes to construct the eigengene network. Hierarchical clustering was used to visualize the

relationship between the rejection phenotypes. We correlated the WGCNA module eigengene with ISHLT and unsupervised classification assignments.

Agreement analysis among pathologists on the histological grading was performed using weighted kappa coefficients with 95% confidence intervals. The assignment probability derived from the unsupervised classification was used to predict ISHLT. Receiver operating characteristic curves (ROC) and the area under the curve (AUC) were computed. Circulating plasma cytokine was compared between the ISHLT and unsupervised classification classes using general linear models adjusted for age and sex. Similar cytokines profiles were clustered together following the “pheatmap” algorithm in R. BNP levels were compared among groups using the Kruskal-Wallis test and Mann Whitney U test as appropriate. Further statistical details are provided in the Supplementary Material.

RESULTS

Patient population and samples

A total of 64 tissue samples were obtained from 47 patients. The mean age of the study population was 50.0 (SD14.7) years; 70% of the population was male and 70% were of European ancestry (Table 1A). Biopsy samples were collected during the posttransplant surveillance with a median of 67 days (IQR 30–152)]. When formally assessed by the center’s reporting pathologist, 23 samples (36%) were classified as ACR 1R, and 11 samples (17%) as ACR 2R. Table 1B summarizes the characteristics of the EMBs.

Interobserver agreement among pathologists

The hematoxylin-eosin-stained slides evaluated externally in a blinded fashion, showed an overall concordance of <65% between pathologists. In biopsies with 0R, the concordance was ≤93%, ≤74% for 1R, and ≤73% for 2R (Table 2), which aligns with the findings of a more extensive concordance study.[10]

Unsupervised classification and relationship with the ISHLT grades

The optimal transport transformation and class assignment probability of cardiac biopsy specimens, led to their classification into three categories: unsupervised class (UC) 1 (UC1), 2 (UC2), and 3 (UC3). Figures S1 A & B illustrate the procedure through the effect of gene expression on the assignment of samples to classes. Out of the 64 heart tissue samples, 23 (35.9%) were assigned to the UC1, 21 (32.8%) to UC2, and 20 (31.3%) were assigned to UC3. The resulting UC categories and corresponding class assignment probabilities for each sample are listed in Table 3. The ISHLT 0R grade was assigned more frequently to UC1 (47%). The 1R grade was often assigned to UC1 (39%) and UC2 (35%). Conversely, 2R was more frequently assigned to UC2 (72%) with the highest median probability. The UC3 shared frequency characteristics with all ISHLT grades.

Although the aim of this study was to develop a molecular classification not dependent on traditional histology grades. For comparison purposes, we also assessed the performance of the developed UC to predict ISHLT grades. The AUC was 0.67 for grade 0R; 0.74 for 1/2R; and 0.77 for 2R (Figure 2). These results may reflect a degree of inconsistency

between histological interpretations and underlying molecular activity, echoing findings from Halloran's Molecular Microscope.[14]

Gene expression profiles among the unsupervised classification and ISHLT grades

The WGCNA analysis resulted in a network composed of 16 modules with sizes ranging from 86 to 3348 genes. Among the 16 gene modules, eight had the highest module-trait relationships, with stronger correlation values (Figure S2–S4). The module-trait relationships for the eight modules, biological processes, and the 10 top scoring hub genes are summarized in Figure 3.

Gene modules were predominately enriched by gene ontology (GO) processes and pathways related to cardiac/mitochondrial function, immune function, and tissue injury response. Four gene modules (green-yellow, salmon, blue, and midnight-blue) were mainly enriched by genes encoding proteins involved in cardiac contractility, response to oxidative stress, mitochondrial function, substrate metabolism, and energy generation. Two modules (turquoise and green) were predominantly related to innate and adaptive immune response pathways, leukocyte activation, T- and B- cell proliferation, antigen processing and presentation, and cytokine regulation. Two modules (magenta and purple) were enriched with GO categories associated with extracellular matrix organization, endothelium development, muscle cell differentiation, DNA damage checkpoint, fibroblast proliferation, and tissue development.

Overall, UC molecular signatures had similarities to ISHLT grading. However, module-trait correlations were stronger for the developed UC than for histologic grades. UC1 samples resembled molecular signatures of 0R, highly enriched for expressed genes related to mitochondrial activity (corr. 0.74, $p= 3.0 \times 10^{-12}$); and low activity of enriched genes related to immune function (corr. −0.51, $p= 2.0 \times 10^{-5}$). UC2 samples shared characteristics of 2R, strongly enriched for genes related to immune function (corr. 0.78, $p= 5.0 \times 10^{-14}$); and decreased activity of enriched genes related to mitochondrial function (corr. −0.56, $p= 1.0 \times 10^{-6}$). UC3 samples shared characteristics of UC 1 and 2, less defined by their mitochondrial or immune response activity; and with decreased gene module activities observed in the UC1 and UC2, thus sharing some of the features observed in the UC1 and UC2 samples (Figure 3). Thus, the new unsupervised classification resulted in stronger correlations with functional gene modules, suggesting a better depiction of the underlying biology.

BNP and Cytokine profiling

Cytokine (n=19) and BNP (n=30) were tested at the time of biopsy. We found nine differentially expressed cytokines among the UC classes and eight cytokines among the ISHLT classification. The cytokine profiles of the differentially expressed cytokines are shown in Figure 4. Heat map profiles were clustered together, UC 1 and 0R shared similar profiles with lower levels of cytokines compared to UC2and 1/2R. In contrast, UC2 and 1/2R shared a similar pattern with higher levels of cytokines. UC3 had a pattern partially close to 1/2R. Cytokines with testing values for each class are described in Table S1. Analysis performed following the developed UC showed that BNP levels between the UC

groups were statistically different (overall p value of 0.02), and UC2 had the highest BNP levels (Figure 5A). Pairwise comparisons revealed significant differences between UC2 and UC1 (p=0.02). Similarly, we found higher BNP levels in 1/2R compared to 0R. However, this difference was not statistically significant (p=0.37) (Figure 5B). Hence, significant levels of cytokines (p= <0.05) were detected in one of the unsupervised classes (UC2). Furthermore, UC2 exhibited higher levels of BNP (p<0.05).

DISCUSSION

The main results of the present study are that we proposed a gene expression-based classification of EMBs that is not reliant on histological interpretations, while also adjusting for factors that influence gene expression in transplantation. Three cluster groups were assigned, UC1, UC2, UC3. The UC2 cluster was more likely to be associated with 1R and 2R (Table 3), displayed a strong immune activation in gene expression profiles (Figure 3), showed an inflammatory cytokine profile (Figure 4), and had higher BNP levels (Figure 5). Hence, utilizing EMB molecular assessments alone have the potential to evaluate for rejection, which is a step towards reducing operator dependence. Additionally, the study found less than 65% overall agreement in histological interpretations, reflecting the know variability due to operator-dependent nature (Table 2). An important problem, given that based on the current standards, a considerable number of patients are at risk of suboptimal rejection diagnosis.[8,10]

The Unsupervised mRNA-seq classification and its relationship with ISHLT grades

Specimens graded as 0R had the highest-class assignment probabilities for UC1, and 2R had the highest probability of being assigned to UC2 (Table 3). The gene expression classification showed differences to the ISHLT grades, with moderate AUC performance results (Figure 2). This was expected and reflects the known variability in the histological interpretation that was also observed in this study. Results from Halloran's Molecular Microscope further support these findings. Halloran *et al*[14] developed an unsupervised archetype classification based on gene expression. Histological-molecular discrepancies were reported with an AUC of 0.65 to predict T cell-mediated rejection. Taken together, these finding suggest that the ISHLT grading may not represent the underling allograft rejection biology consistently due to the variability in histological interpretations.

Biological functions underling the Unsupervised mRNA-seq classification and ISHLT grades

Gene module-trait relationships and hub gene function results (Figure 3) indicated that UC1 was closely related to ISHLT 0R: (1) suppressed immune response related gene expression, (2) increased activity of cardiac/mitochondrial function-related genes, and (3) decreased activity of genes related to injury response. Conversely, UC2 resembled ISHLT 2R in the following ways: (1) increased activity of immune related genes, (2) decreased activity of cardiac/mitochondrial function-related genes, and (3) increased activity of injury response genes. The UC3 shared characteristics of UC 1 and 2. Overall, compared to ISHLT the molecular activity was more evident in the UC, with a stronger correlation with

functional gene modules (i.e. several correlations ≥0.5 or ≤−0.5), suggesting an improved representation of the underlying mechanistic processes and pathways.

Cytokine and BNP levels in the context of the Unsupervised mRNA-seq classification

Cytokine profiling results suggested that inflammatory profiles can be distinguished in UC2 and 3 with higher level of cytokines (Figure 4). Briefly, cytokines such as IL-12 influence the proliferation of T lymphocytes.[29] The FGF-2 diminishes cardiac remodeling.[30] The G-CSF is associated with decreased incidence of acute rejection.[31] Interestingly, IFN-a2, IL-2, IL-7, and IL-9 have been associated to cardiovascular adverse effects and allograft rejection.[32–35] Following the ISHLT classification, 1R and 2R had elevated levels of cytokines, with similar number of significant cytokines detected. BNP analysis revealed significantly elevated BNP levels related to UC2. We also found elevated levels of 1/2R; however, this was not statistically significant (Figure 5). In summary, although limited by sample size, in UC2, we observed a cytokine inflammatory profile and high BNP levels, suggesting allograft rejection in the context of cardiac dysfunction and an inflammatory state.

The Unsupervised mRNA-seq classification and the Molecular Microscope System for EMB evaluations independent of histological interpretations

The Molecular Microscope System is in line with the goal of our investigation, which is to evaluate EMBs without relying on histology interpretations.[14] Halloran *et al.* developed rejection-associated transcripts to classify rejection archetype clusters. Three archetypes were identified, no rejection, T cell-mediated rejection, and antibody mediated rejection. Incongruences between the histological and molecular results were also observed, with moderate AUC scores. Nonetheless, there exist differences between the Molecular Microscope and the study reported here. (1) the molecular microscope used Microarray Technology (Affymetrix), which is based on array based nucleic acid probes which have significant limitations including limited dynamic range, increased background noise, off-target binding and signal saturation. In our analysis, RNA-Seq was used which provides a broader dynamic range and more accurate quantification of gene expression versus array based expression platforms. (2) The molecular microscope pipeline followed an unsupervised approach (principal component analysis) to cluster rejection groups independently of histology assessments. In contrast, our study team followed the *optimal transport* pipeline which also uses an unsupervised classification methodology. (3) The molecular microscope used rejection-associated transcripts from kidney transplant to guide the development of the heart transplant rejection diagnostic system. In our study, we did not use external information to guide the cluster classification. The *optimal transport* and the unsupervised cluster methodology used, was specially considered for heart transplant rejection to control known factors affecting the variability of gene expression. However, both studies are challenging the traditional ISHLT evaluation, a major limitation for validation is the lack of a reliable reference framework (gold standard). Relying solely on histological assessments for validation would restrict technological advancements. Given the interpretation variability, the ISHLT system cannot always be assumed to be accurate, and alternative standards of reference are necessary. Future validation studies should focus on alternative reference standards such as immunosuppression use, graft dysfunction, cardiac

allograft vasculopathy, re-transplantation, or mortality (clinical and outcome references). Biomarker references can include donor-derived cell-free DNA, circulating mononuclear cell gene expression profiling, and microRNAs. The use of alternative standards of reference has been recently explored in kidney and heart transplant rejection.[36,37] Large prospective studies that incorporate clinical outcomes or composite outcomes with biomarkers will be necessary to determine whether intragraft molecular classifications can be validated as a more accurate means of identifying rejection.

Limitations

Although our sample size is relatively small, the methodology employed is well-suited for relatively modest sample sizes, as it enables diagnosing one sample at a time in a sequential fashion. Each sample is taken as a testing case and used the remaining ones for training.[23] Additionally, the sample size used is it is in line with other intragraft gene expression profile studies.[11,12] The approach is easily scalable and larger studies would yield more robust evidence in the future. This study did not cover the heterogenous spectrum of pathological diagnoses related to rejection (e.g., severe ACR, antibody mediated, mixed). The proposed gene expression-based classification needs to be validated in well-powered prospective studies using clinical outcomes or composite outcomes with biomarkers for allograft rejection. The current study included the transcriptional profiling of EMBs, which comprised several different cell types. Therefore, expression analysis cannot be used to delineate the cell types responsible for gene expression. This biological limitation will eventually need to be addressed in future studies by isolating cardiomyocytes, endothelial cells, fibroblasts, and immune cells, and analyzing their gene expression levels.

Conclusion

An unsupervised mRNA-seq classification for EMBs was developed with stronger representation of different biological processes compared to the ISHLT histological classification. The proposed classification revealed a strong immune activation in gene expression profiles and significant cytokine and BNP levels, supporting findings in a clinical context. If further validated, the unsupervised mRNA-seq classification could provide more objective EMBs evaluations, reducing operator dependence interpretation.

Supplementary Material

Refer to Web version on PubMed Central for supplementary material.

Acknowledgements and Funding

The authors acknowledge the important work and contributions of Eleanor Chang B.S. in this study. This work was funded by the American Heart Association grant 11GRNT7990092, and NIH grant 1R01AI144522–01A1.

Abbreviations:

ACR	acute cellular rejection
AMR	antibody-mediated rejection

ATP	adenosine triphosphate
AUC	area under the curve
BMP	bone morphogenetic proteins
BNP	B-type natriuretic peptide
cAMP	cyclic adenosine monophosphate
CD	cluster of differentiation
EMB	endomyocardial biopsies
ERAD	endoplasmic-reticulum-associated protein degradation
ETC	electron transport chain
FGF	Fibroblast growth factor
G-CSF	Granulocyte colony-stimulating factor
GO	gene ontology
IFN	Interferon
IL	interleukin
IRB	Institutional review board
ISHLT	International Society of Heart and Lung Transplantation
MHC	major histocompatibility complex
mRNA-seq	mRNA sequencing
NFKB	nuclear factor kappa B
NK	natural killer
ROC	receiver operating characteristic
UAB	University of Alabama at Birmingham, Alabama
UC	unsupervised class
UCLA	University of California, Los Angeles
WGCNA	weighted gene co-expression network analysis

REFERENCES

1. Lund LH, Edwards LB, Kucheryavaya AY, et al. The registry of the International Society for Heart and Lung Transplantation: thirty-first official adult heart transplant report--2014; focus theme: retransplantation. J Heart Lung Transplant. 2014;33(10):996–1008. doi:10.1016/j.healun.2014.08.003 [PubMed: 25242124]

2. Pober JS, Chih S, Kobashigawa J, Madsen JC, Tellides G. Cardiac allograft vasculopathy: current review and future research directions. Cardiovascular Research. 2021;117(13):2624–2638. doi:10.1093/cvr/cvab259 [PubMed: 34343276]

3. Khush KK, Hsich E, Potena L, et al. The International Thoracic Organ Transplant Registry of the International Society for Heart and Lung Transplantation: Thirty-eighth adult heart transplantation report - 2021; Focus on recipient characteristics. J Heart Lung Transplant. 2021;40(10):1035–1049. doi:10.1016/j.healun.2021.07.015 [PubMed: 34419370]

4. Khush KK, Cherikh WS, Chambers DC, et al. The International Thoracic Organ Transplant Registry of the International Society for Heart and Lung Transplantation: Thirty-sixth adult heart transplantation report - 2019; focus theme: Donor and recipient size match. J Heart Lung Transplant. 2019;38(10):1056–1066. doi:10.1016/j.healun.2019.08.004 [PubMed: 31548031]

5. Stewart S, Winters GL, Fishbein MC, et al. Revision of the 1990 working formulation for the standardization of nomenclature in the diagnosis of heart rejection. J Heart Lung Transplant. 2005;24(11):1710–1720. doi:10.1016/j.healun.2005.03.019 [PubMed: 16297770]

6. Berry GJ, Burke MM, Andersen C, et al. The 2013 International Society for Heart and Lung Transplantation Working Formulation for the standardization of nomenclature in the pathologic diagnosis of antibody-mediated rejection in heart transplantation. J Heart Lung Transplant. 2013;32(12):1147–1162. doi:10.1016/j.healun.2013.08.011 [PubMed: 24263017]

7. Veiga Barreiro A, Crespo Leiro M, Doménech García N, et al. Severe cardiac allograft dysfunction without endomyocardial biopsy signs of cellular rejection: incidence and management. Transplant Proc. 2004;36(3):778–779. doi:10.1016/j.transproceed.2004.03.033 [PubMed: 15110660]

8. Marboe CC, Billingham M, Eisen H, et al. Nodular endocardial infiltrates (Quilty lesions) cause significant variability in diagnosis of ISHLT Grade 2 and 3A rejection in cardiac allograft recipients. J Heart Lung Transplant. 2005;24(7 Suppl):S219–226. doi:10.1016/j.healun.2005.04.001

9. Bhalodolia R, Cortese C, Graham M, Hauptman PJ. Fulminant acute cellular rejection with negative findings on endomyocardial biopsy. J Heart Lung Transplant. 2006;25(8):989–992. doi:10.1016/j.healun.2006.04.002 [PubMed: 16890123]

10. Crespo-Leiro MG, Zuckermann A, Bara C, et al. Concordance among pathologists in the second Cardiac Allograft Rejection Gene Expression Observational Study (CARGO II). Transplantation. 2012;94(11):1172–1177. doi:10.1097/TP.0b013e31826e19e2 [PubMed: 23222738]

11. Holweg CTJ, Potena L, Luikart H, et al. Identification and Classification of Acute Cardiac Rejection by Intragraft Transcriptional Profiling. Circulation. 2011;123(20):2236–2243. doi:10.1161/CIRCULATIONAHA.109.913921 [PubMed: 21555702]

12. Bodez D, Hocini H, Tchitchek N, et al. Myocardial Gene Expression Profiling to Predict and Identify Cardiac Allograft Acute Cellular Rejection: The GET-Study. PLoS One. 2016;11(11):e0167213. doi:10.1371/journal.pone.0167213 [PubMed: 27898719]

13. Loupy A, Duong Van Huyen JP, Hidalgo L, et al. Gene Expression Profiling for the Identification and Classification of Antibody-Mediated Heart Rejection. Circulation. 2017;135(10):917–935. doi:10.1161/CIRCULATIONAHA.116.022907 [PubMed: 28148598]

14. Halloran PF, Potena L, Huyen JPDV, et al. Building a tissue-based molecular diagnostic system in heart transplant rejection: The heart Molecular Microscope Diagnostic (MMDx) System. The Journal of Heart and Lung Transplantation. 2017;36(11):1192–1200. doi:10.1016/j.healun.2017.05.029 [PubMed: 28662985]

15. Afzali B, Chapman E, Racapé M, et al. Molecular Assessment of Microcirculation Injury in Formalin-Fixed Human Cardiac Allograft Biopsies With Antibody-Mediated Rejection. American Journal of Transplantation. 2017;17(2):496–505. doi:10.1111/ajt.13956 [PubMed: 27401781]

16. Piening BD, Dowdell AK, Zhang M, et al. Whole transcriptome profiling of prospective endomyocardial biopsies reveals prognostic and diagnostic signatures of cardiac allograft rejection. J Heart Lung Transplant. Published online February 3, 2022:S1053-2498(22)01394-8. doi:10.1016/j.healun.2022.01.1377

17. Scherer A. Batch Effects and Noise in Microarray Experiments: Sources and Solutions. John Wiley & Sons; 2009.

18. Schaenman JM, Rossetti M, Lum E, et al. Differences in Gene Expression in Older Compared With Younger Kidney Transplant Recipients. Transplant Direct. 2019;5(4):e436. doi:10.1097/TXD.0000000000000870 [PubMed: 30993190]
19. Christakoudi S, Runglall M, Mobillo P, et al. Development and validation of the first consensus gene-expression signature of operational tolerance in kidney transplantation, incorporating adjustment for immunosuppressive drug therapy. eBioMedicine. 2020;58. doi:10.1016/j.ebiom.2020.102899
20. Mehra MR, Kobashigawa JA, Deng MC, et al. Transcriptional signals of T-cell and corticosteroid-sensitive genes are associated with future acute cellular rejection in cardiac allografts. J Heart Lung Transplant. 2007;26(12):1255–1263. doi:10.1016/j.healun.2007.09.009 [PubMed: 18096476]
21. Trigila G, Tabak EG. Data-Driven Optimal Transport. Communications on Pure and Applied Mathematics. 2016;69(4):613–648. doi:10.1002/cpa.21588
22. Tabak EG, Trigila G. Explanation of Variability and Removal of Confounding Factors from Data through Optimal Transport. Communications on Pure and Applied Mathematics. 2018;71(1):163–199. doi:10.1002/cpa.21706
23. Agnelli JP, Cadeiras M, Tabak EG, Turner CV, Vanden-Eijnden E. Clustering and Classification through Normalizing Flows in Feature Space. Multiscale Model Simul. 2010;8(5):1784–1802. doi:10.1137/100783522
24. Tabak EG, Turner CV. A Family of Nonparametric Density Estimation Algorithms. Communications on Pure and Applied Mathematics. 2013;66(2):145–164. doi:10.1002/cpa.21423
25. Romero E, Chang E, Tabak E, et al. Rejection-associated Mitochondrial Impairment After Heart Transplantation. Transplantation Direct. 2020;6(11):e616. doi:10.1097/TXD.0000000000001065 [PubMed: 33134492]
26. Langfelder P, Horvath S. WGCNA: an R package for weighted correlation network analysis. BMC Bioinformatics. 2008;9(1):559. doi:10.1186/1471-2105-9-559 [PubMed: 19114008]
27. Shannon P, Markiel A, Ozier O, et al. Cytoscape: a software environment for integrated models of biomolecular interaction networks. Genome Res. 2003;13(11):2498–2504. doi:10.1101/gr.1239303 [PubMed: 14597658]
28. Chin CH, Chen SH, Wu HH, Ho CW, Ko MT, Lin CY. cytoHubba: identifying hub objects and sub-networks from complex interactome. BMC Systems Biology. 2014;8(4):S11. doi:10.1186/1752-0509-8-S4-S11 [PubMed: 25521941]
29. Teng MWL, Bowman EP, McElwee JJ, et al. IL-12 and IL-23 cytokines: from discovery to targeted therapies for immune-mediated inflammatory diseases. Nat Med. 2015;21(7):719–729. doi:10.1038/nm.3895 [PubMed: 26121196]
30. Svystonyuk DA, Ngu JM, Mewhort HE, et al. Fibroblast growth factor-2 regulates human cardiac myofibroblast-mediated extracellular matrix remodeling. J Transl Med. 2015;13:147. doi:10.1186/s12967-015-0510-4 [PubMed: 25948488]
31. Vrtovec B, Haddad F, Pham M, et al. Granulocyte colony-stimulating factor therapy is associated with a reduced incidence of acute rejection episodes or allograft vasculopathy in heart transplant recipients. Transplant Proc. 2013;45(6):2406–2409. doi:10.1016/j.transproceed.2013.01.106 [PubMed: 23953556]
32. Teragawa H, Hondo T, Amano H, Hino F, Ohbayashi M. Adverse effects of interferon on the cardiovascular system in patients with chronic hepatitis C. Jpn Heart J. 1996;37(6):905–915. doi:10.1536/ihj.37.905 [PubMed: 9057685]
33. Chen H, Yang J, Zhang S, et al. Serological cytokine profiles of cardiac rejection and lung infection after heart transplantation in rats. Journal of Cardiothoracic Surgery. 2019;14(1):26. doi:10.1186/s13019-019-0839-5 [PubMed: 30696462]
34. Racapé M, Vanhove B, Soulillou JP, Brouard S. Interleukin 7 receptor alpha as a potential therapeutic target in transplantation. Arch Immunol Ther Exp (Warsz). 2009;57(4):253–261. doi:10.1007/s00005-009-0036-7 [PubMed: 19585222]
35. Assadiasl S, Fatahi Y, Nicknam MH. T helper-9 cells and Interleukin-9 in transplantation: The open question. Human Immunology. Published online March 18, 2022. doi:10.1016/j.humimm.2022.03.006

36. Schachtner T, von Moos S, Kokkonen SM, et al. The Molecular Diagnosis Might Be Clinically Useful in Discrepant Kidney Allograft Biopsy Findings: An Analysis of Clinical Outcomes. Transplantation. 2023;107(2):485. doi:10.1097/TP.0000000000004284 [PubMed: 36117252]

37. Madill-Thomsen KS, Reeve J, Aliabadi-Zuckermann A, et al. Assessing the Relationship Between Molecular Rejection and Parenchymal Injury in Heart Transplant Biopsies. Transplantation. 2022;106(11):2205. doi:10.1097/TP.0000000000004231 [PubMed: 35968995]

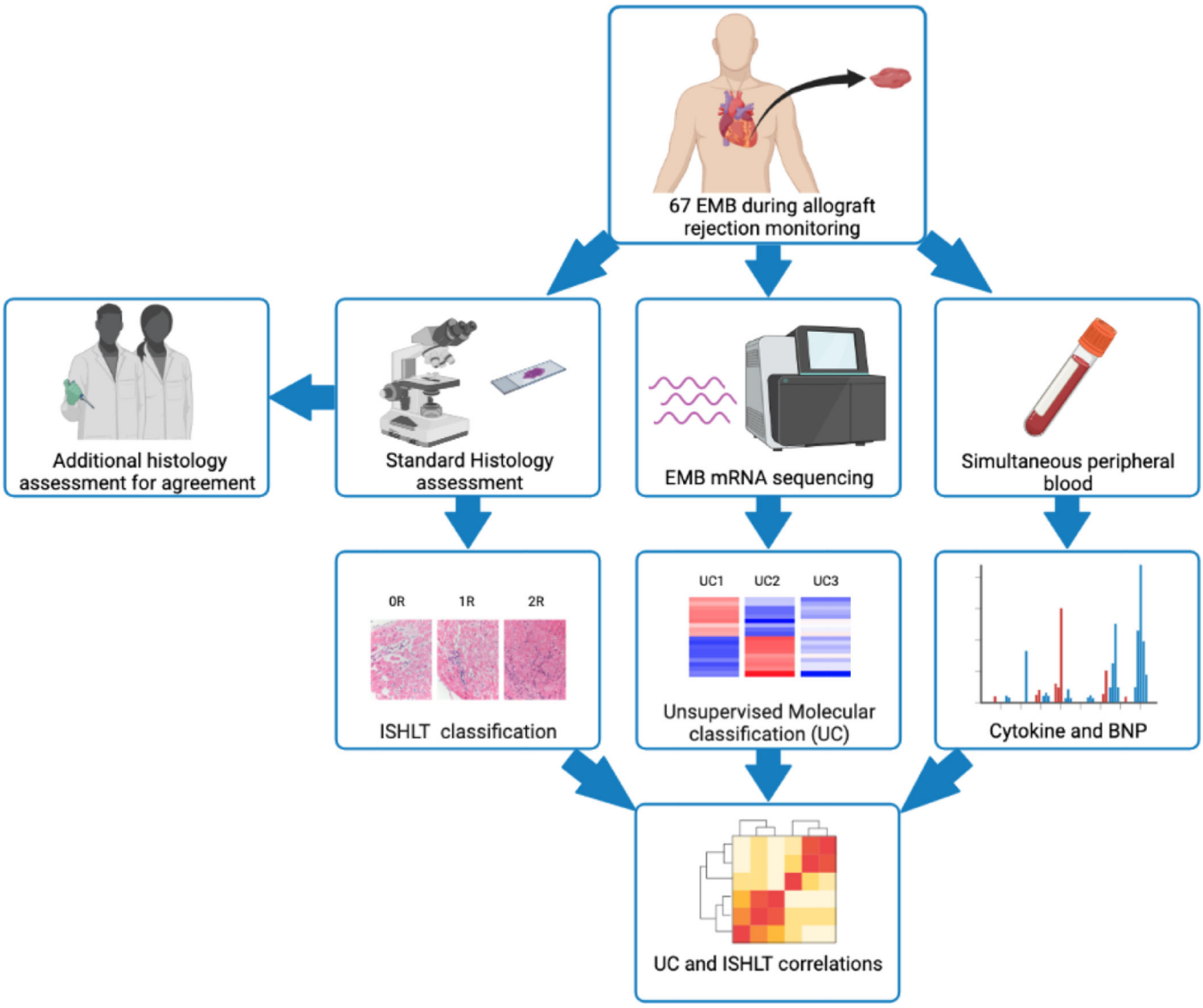

Figure 1. Study design overview.

Endomyocardial biopsies (EMB) were collected during rejection surveillance, then the EMBs were subjected to mRNA sequencing. EMBs were classified following a new proposed classification based on gene expression alone without relying on histology interpretation. Comparisons were made between the proposed classification and cytokines, natriuretic peptides, as well as ISHLT grades. Agreement analysis was conducted to assess the variability in histology evaluations by comparing the assessments of the center and two blinded external pathologists. Abbreviations: ISHLT, International Society of Heart and Lung Transplantation; UC, Unsupervised classification. Tissue image modified from Van Aelst et al. Figure created with BioRender.com.

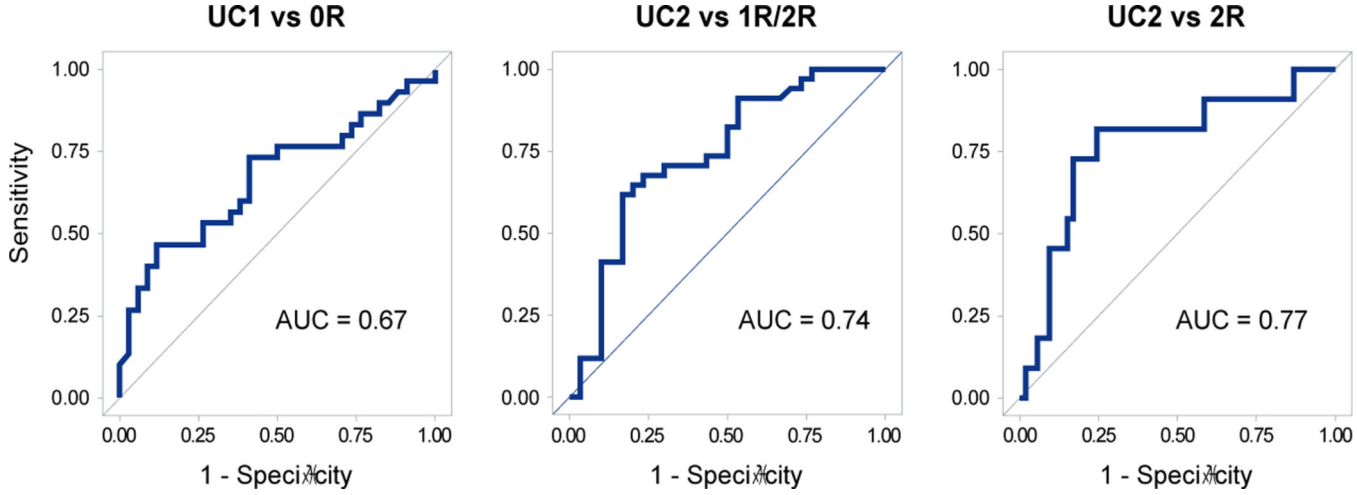

Figure 2. ROC curve for UC assignment probability against ISHLT 0R, 1/2R or 2R.

Comparison of the molecular classifications against the ISHLT grades resulted in moderate AUC scores, suggesting a degree of inconsistency between histological and molecular assessments. Abbreviations: ROC, receiver-operating characteristic; UC, Unsupervised classification; ISHLT, International Society of Heart and Lung Transplantation.

Gene Module-EMB Class Relationship

Related function (gene module)		Processes and pathways	Hub Genes	0R	1R	2R	UC1	UC2	UC3
CARDIAC	Cardiac Function (greenyelow)	Regulation of cardiac contraction, regulation of vasoconstriction, cAMP-mediated signaling, right ventricle morphogenesis, heat shock protein binding, ERAD pathway, regulation of muscle tissue development	*AKT2, ARAF, BAG6, KLHL21, LONP1, MYH14, PNPLA2, PPP1R13L, TBC1D17, USF2*	0.01 (0.9)	0.16 (0.2)	−0.22 (0.08)	0.62 (4e−08)	−0.22 (0.08)	−0.42 (5e−04)
	Response to Cellular Stress (salmon)	Response to unfolded protein, Golgi vesicle transport, receptor metabolic process, organelle disassembly, positive regulation of nitric oxide biosynthetic process	*ADD1, AP2A1, BAG3, CTSD, KLC2, MEF2D, PCBP1, PRKACA, STK25, SYNPO*	0.12 (0.3)	0.092 (0.5)	−0.28 (0.03)	0.58 (5e−07)	−0.047 (0.7)	−0.55 (2e−06)
	Mitochondrial Function 1 (blue)	Generation of precursor metabolites and energy, negative regulation of oxidative stress induced cell death, mitochondrial membrane organization, striated muscle contraction	*ACO2, ALDH2, ATP5B, FH, MAPKAPK3, NDUFV1, PDK2, PEBP1, SDHA, UQCRC1*	0.17 (0.2)	−0.0076 (1)	−0.21 (0.1)	0.74 (3e−12)	−0.56 (1e−06)	−0.2 (0.1)
	Mitochondrial Function 2 (midnightblue)	Nuclear transcribed mRNA catabolic process, mitochondrial ATP synthesis coupled electron transport, purine nucleotide metabolic process, regulation of tumor necrosis factor production, regulation of intrinsic apoptotic signaling pathway, ribosome biogenesis, cellular response to toxic substance.	*ATP5O, AURKAIP1, COX14, COX4I1, MYEOV2, NDUFA4, NDUFB8, NDUFV2, RPL23A, UQCR11*	0.034 (0.8)	0.019 (0.9)	−0.07 (0.6)	0.48 (6e−05)	−0.086 (0.5)	−0.41 (7e−04)
IMMUNE	AlloImmune Response (turquoise)	Myeloid cell development, T-Cell Co-stimulation, T-Cell and B-Cell proliferation, leukocyte apoptosis, Antigen processing and presentation through MHC-II, Leukocyte migration, NK cell mediated cytotoxicity, IFN-gamma and cytokine production including IL-4, IL 10, IL-12, and IL-15.	*CD53, CTSS, HLADRA, IRF8, PTPRC, RAC2, IL10RA, HLA_DPB1, CD84, MS4A6A*	−0.36 (0.004)	0.049 (0.7)	0.41 (7e−04)	−0.51 (2e−05)	0.78 (5e−14)	−0.26 (0.04)
	Inflammation (green)	Collagen metabolic process, regulation of neurotransmitter levels, synaptic vesicle transport and synapse organization, smooth muscle contraction, coagulation, IL-8, endothelial cell migration, chemokine activity, BMP signaling, response to TGB-beta, cell substrate adhesion.	*ANXA1, ANXA2, ANXA2P2, ATP1B3, FN1, MICALL2, SERP1, SH3BGRL, TAGLN2, TFPI*	−0.091 (0.5)	0.032 (0.8)	0.08 (0.5)	−0.38 (0.002)	0.64 (1e−08)	−0.26 (0.04)
INJURY	Tissue injury and repair 1 (magneta)	Extracellular matrix, endothelium development, muscle cell differentiation, NFKB and Notch signaling, DNA damage checkpoint, platelet activation, epithelial cell apoptosis, endochondral bone morphogenesis.	*AGRN, CHERP, FAM65A, GNAI2, PIP5K1C, PLD3, POLR2A, PRAF2, TNFSF12, ZYX*	−0.097 (0.4)	0.14 (0.3)	−0.055 (0.7)	0.2 (0.1)	0.32 (0.01)	−0.53 (7e−06)
	Tissue injury and repair 2 (purple)	Fibroblast proliferation, osteoblast differentiation, regulation of smoothened signaling pathways, endocardial cushion morphogenesis, extracellular matrix, cyclooxygenase pathway and doxorubicin, progesterone, retinoid and prostaglandin metabolic processes.	*AKAP12, AKR1C3, BGN, COL6A1, FBLN2, FBLN5, IL33, SERPING1, TCF21, TIMP2*	−0.0012 (1)	0.046 (0.7)	−0.057 (0.7)	−0.21 (0.09)	0.34 (0.006)	−0.12 (0.3)

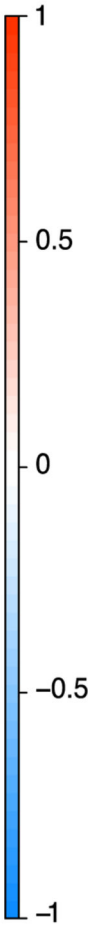

Figure 3. Gene modules, processes, hub genes, and UC or ISHLT class correlations.

Compared to ISHLT, the proposed UC has several strong correlations with functional gene modules (correlation ≥0.5 or ≤−0.5). The color gradient denotes the gene module to UC or ISHLT class correlation coefficient, each cell depicts the correlation value (top) and p-value (bottom). Abbreviations: UC, unsupervised classification; cAMP, cyclic adenosine monophosphate; ERAD, endoplasmic-reticulum-associated protein degradation; ATP, adenosine triphosphate; MHC, major histocompatibility complex; IFN, interferon; IL, interleukin; NK, natural killer; BMP, bone morphogenetic protein; NFKB, nuclear factor kappa B.

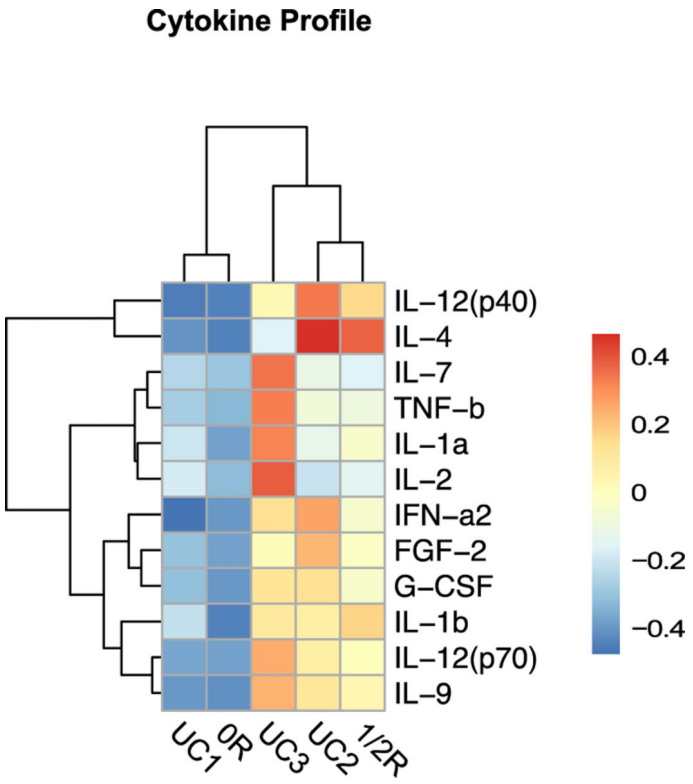

Figure 4. Significant cytokines following the UC and ISHLT classification.

Cytokine profiling showed that different cytokines were found at significant levels (p=<0.5) following the developed UC. Heatmap depicts significant cytokines within the UC and ISHLT groups. Similar heat map profiles were clustered together following the “pheatmap” algorithm. The heatmaps are scaled to z-score and box colors represent mean levels.

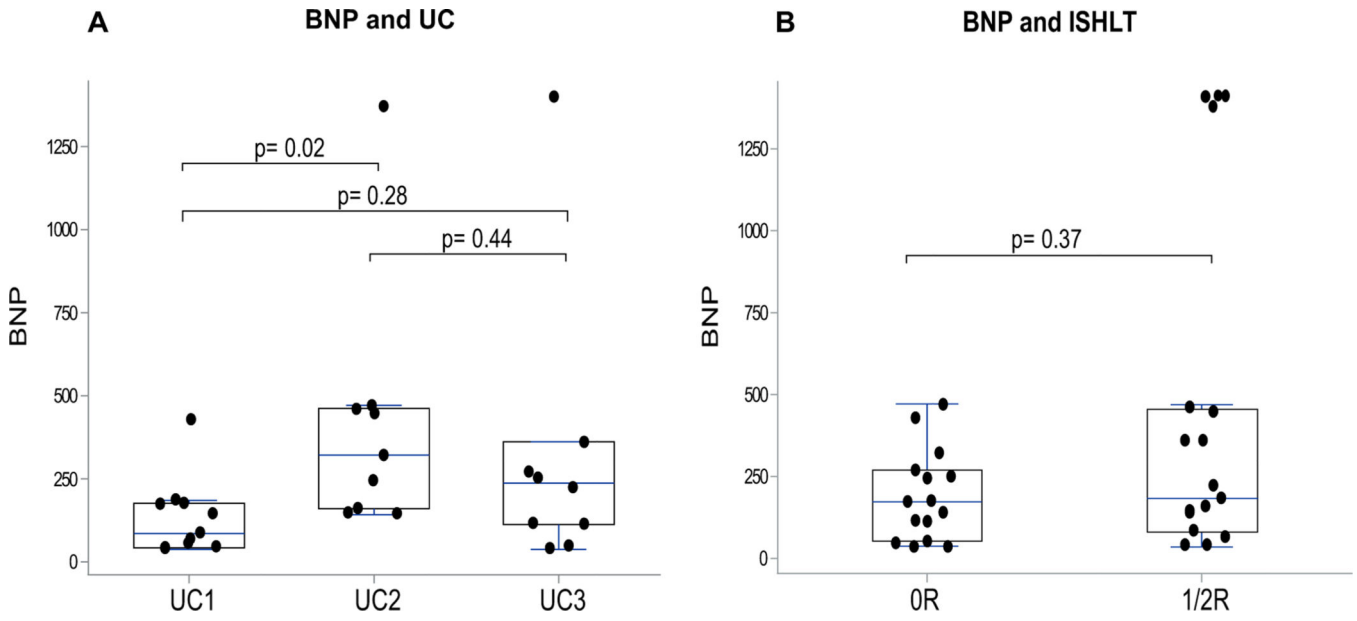

Figure 5. BNP levels following the UC and ISHLT classification.

(**A**) BNP levels between the UC groups shown that UC2 class had significantly higher BNP levels compared with UC1 (p= 0.02). (**B**) The BNP levels between ISHLT class 1/2R and 0R were not statistically significant (p=0.37). Abbreviations: BNP, B-type natriuretic peptide; ISHLT, International Society of Heart and Lung Transplantation; UC, Unsupervised classification.

Table 1A.

Characteristics of study population

Demographics	*n*= 47
Age, (years) mean (±SD)	50.0 (±14.7)
Sex, Male	33 (70.2)
Race, no. (%)	
Caucasian	33 (70.2)
African American	6 (12.8)
Filipino	2 (4.3)
Asian	1 (2.1)
Other	5 (10.6)
EMB description	*n*= 64
Samples per patient, no. (%)	
1 Sample	35 (74.5)
2 Samples	10 (21.3)
3 Samples	1 (2.1)
6 Samples	1 (2.1)
Histopathology grading ACR, no. (%)	
0R	30 (46.9)
1R	23 (35.9)
2R	11 (17.2)
Batches, no. (%)	
Batch 1 (UCLA)	30 (46.9)
Batch 2 (UAB)	20 (31.3)
Batch 3 (UAB)	14 (21.9)

Abbreviations: ACR, acute cellular rejection; EMB, endomyocardial biopsy; UAB, University of Alabama at Birmingham; UCLA, University of California Los Angeles.

Table 1B.

Characteristics of the EMBs

Characteristics[a]	ACR 0R (*n*=30)	ACR 1R (*n*=23)	ACR 2R (*n*=11)
Age	55 (45–60)	55 (40–59)	54 (41–67)
Sex, Male	21 (70)	15 (65.2)	10 (90.9)
Race			
White	19 (63.3)	14 (60.9)	9 (81.8)
Black	3 (10)	3 (13)	2 (18.2)
Other	8 (26.7)	6 (26.1)	0
Ethnicity			
Non-Hispanic	24 (80)	15 (65.2)	11 (100)
Hispanic	6 (20)	8 (34.8)	0
LVEF, %	55 (55–57.5)	55 (55–57.5)	55 (55–55)
BNP, pg/mL	173 (53–269)	172.5 (85–361)	1410(1410–1410)
MMF Dose, mg	2000 (2000–2000)	2000 (2000–2000)	2000 (2000–2000)
Pr Dose, mg	13 (10–19)	15.5 (7.5–20)	10 (7.5–20)
Tacrolimus level, ng/mL	11.6 (7.6–13.2)	8.3 (7.6–10.4)	7.7 (5.9–13.7)
Quilty Effect			
Quilty effect A	6.0 (20.0)	4 (17.4)	0
Quilty effect B	2.0 (6.7)	2 (8.7)	0
HLA DSA			
DSA+	12.0 (40)	6 (26.1)	4 (36.4)

[a]Data presented as median (IQR) or n (%).

Abbreviations: ACR, acute cellular rejection; AMR, antibody-mediated rejection; BNP, brain natriuretic peptide; DSA, donor-specific HLA antibodies; UAB, University of Alabama at Birmingham; UCLA, University of California Los Angeles; HLA, human leukocyte antigens; LVEF, left ventricular ejection fraction; MMF, mycophenolate; Pr, prednisone.

TABLE 2.

Concordance between ISHLT grades assigned by the center and external blinded pathologists (n=64)

	Blinded Pathologist #1				
Center Pathologist	0R	1R	2R	Ungraded[a]	Agreement (95% CI)[b]
0R	28 (93.3)	2 (6.7)	0	0	
1R	7 (30.4)	16 (69.6)	0	0	0.55 (0.37–0.71)
2R	3 (27.3)	5 (45.5)	3 (27.3)	0	
	Blinded Pathologist #2				
Center Pathologist	0R	1R	2R	Ungraded[a]	
0R	21 (70)	7 (23.3)	2 (6.7)	0	
1R	2 (8.7)	17 (73.9)	1 (4.4)	3 (13)	0.63 (0.46–0.80)
2R	0	2 (18.2)	8 (72.7)	1 (9)	
	Blinded Pathologist #2				
Blinded Pathologist #1	0R	1R	2R	Ungraded[a]	
0R	22 (57.9)	13 (34.2)	3 (7.9)	0	
1R	1 (4.4)	13 (56.5)	6 (26)	3 (13)	0.37 (0.19–0.54)
2R	0	0	2 (66.7)	1 (33.3)	

Cells represent the frequency of ISHLT grades and row percent (%).

[a]Ungraded due to Insufficient sample, Quilty or atypical infiltrate.

[b]kappa coefficient with 95% Confidence Limits.

Table 3.

Probability of molecular class assignment for each sample (n= 64)

	UC, no. (row %)			Probability UC assignment, median (IQR)		
ISHLT	**UC1**	**UC2**	**UC3**	**UC1**	**UC2**	**UC3**
0R	14 (46.7)	5 (16.7)	11 (36.7)	0.14 (0.07–0.91)	0.05 (0.03–0.10)	0.06 (0.05–0.83)
1R	9 (39.1)	8 (34.8)	6 (26.1)	0.12 (0.05–0.80)	0.14 (0.04–0.88)	0.10 (0.04–0.77)
2R	0	8 (72.7)	3 (27.3)	0.05 (0.03–0.07)	0.89 (0.32–0.93)	0.04 (0.03–0.56)

Probability of molecular class assignment for each sample. Abbreviations: ISHLT, International Society of Heart and Lung Transplantation; UC, Unsupervised classification.